Abstract

Objectives: Recently, the trend in treating dental caries relies on preserving the affected dentin. The success of restorations relies on remineralization of affected dentin which is very challenging. Here, we report the facile development of a dual-analogue biomimetic phosphate glass polyacrylate paste (PGPAP), combining two non-collagenous protein precursors [sodium trimetaphosphate (STMP) and polyacrylic acid (PAA)], for remineralization of completely demineralized dentin.

Methods: Human mid-coronal dentin were excessively exposed to an acid challenge for 5h to replicate affected dentin, in which the collagen matrix is not just partially demineralized but also degraded. To increase the challenge, the dentin samples coated with the GPAP were kept in unfavorable mineralization buffer (demineralized water). The extent of de-/remineralization and elemental/chemical composition of dentin were investigated using confocal microscopy, scanning electron microscopy/ energy dispersive X-ray, optical coherence tomography and Infra-red (FTIR).

Results: Dentin, exposed to acidic challenge, showed a frayed and fully demineralized surface layer of 120±30μm with sub-surface partial demineralization of 100-300μm. After 8 weeks of treatment with PGPAP, nearly all dentinal tubules and inter-tubular dentin were completely remineralized with an adherent layer of angular-like crystals. This layer contained Ca, P, Na and Cu and reached 313±6μm in thickness ie, nearly all demineralized dentin becomes remineralized. After 4 weeks, the FTIR spectrum of treated dentin was consistent with native dentin.

Conclusions: The PGPAP might provide a solution towards the remineralization of the affected dentin produced by caries. This might be an ideal scenario for in-situ recapitulation of the original dentin properties towards a pre-carious (native) status.

Key words: Remineralization, Phosphate glass, Sodium trimetaphosphate & Polyacrylic acid

1. Introduction

Recently, a paradigm shift in the treatment of dental caries, the most destructive tooth disease, has emerged [1]. It relies on preserving the remaining tooth structure and the vitality of dental pulp by removing the infected but not affected (non-infected partially demineralized) dentin [1, 2]. Remineralization of affected demineralized dentin is essential for improving the stability of dentin bonding and hence the success of restorations [3]. Remineralization of dentin is very challenging. The presence of some hydroxyapatite crystals as in partially demineralized dentin is an essential requirement for ion-based (classical) remineralization to occur [3-5]. These crystals act as nidi for remineralization [3, 5, 6]. A fluoride-releasing calcium phosphate cement, eg, resin modified glass ionomer, was commonly used for such purpose [7]. Absence of apatite crystals in completely demineralized dentin, however, makes classical remineralization impossible [8]. In such cases, remineralization will occur through organic matrix particle-based process known as "biomineralization". In which, the organic matrix proteins play a fundamental role in apatite nucleation and growth during dentin remineralization [3]. Recently, a new approach, called "biomimetic mineralization", has been used to attempt to imitate the natural process of mineralization. Some hydroxyl ion-releasing cements, (eg, calcium hydroxide [9], mineral trioxide aggregate [10] and Biodentin^{TM} [11, 12]), have been advocated for biomimetic mineralization. They release transforming growth factor (TGF-β1), an essential regulator for dentin repair, after infiltrating and destroying mineralized collagen [13]. Their prolonged contact with mineralized dentin, however, could reduce the integrity of collagen [13]. Furthermore, in most of in vitro remineralization studies, dentin was partially demineralized [14-16] and the treated dentin was immersed in a demineralizing-remineralizing solution that further improves its remineralization

[15-17]. So the outcome will be the result of the remineralizing material as well as the solution used.

Phosphate glasses, as an example of third generation materials, have unique degradation properties in aqueous media. Their constituents are elements naturally present in our body; so no harm would be expected. Once degraded, they release sodium (Na), calcium (Ca) and different phosphate species [18, 19] which are required for remineralization. The released phosphate species are also known for their role in nucleation and apatite layer formation and therefore employed as biomimetic analogue for dentin remineralization [15, 20]. These glasses can be doped with various oxides to induce specific biological functions [21].

Here, we report the facile development of a dual-analogue biomimetic paste for dentin remineralization. This past is based on degradable copper doped phosphate glass (CDPG) and polyacrylic acid (PAA). CDPG has the potential to release copper (Cu) that's known for its antibacterial action [19, 22] in addition to Na, Ca and different phosphate species as mentioned above. PAA has the potential to bind to calcium and phosphate groups present in dentin [23]; it has also been used as a non-collagenous protein (NCP) precursor for dentin remineralization [15, 24]. Throughout this study, the remineralizing potential of this paste was tested against a completely demineralized dentin and the treated dentin samples were kept in distilled water to eliminate any remineralizing potential of the medium. The extent, depth of remineralization as well as the elemental and chemical composition of dentin will be reported.

2. Materials and methods

2.1. Preparation of dentin discs

Discs (1 mm thick) from mid-coronal dentin of extracted human molars were prepared using a low speed diamond saw (Allied, High Tech Products Inc, TECHCUT4) after obtaining ethical approval (no.102-11-17). Dentin discs were polished with # 240 silicon carbide and etched on both sides with 37% phosphoric acid gel for 5 hours, washed and then dried using gentle air. Diagrammatic representation of samples and paste preparation is presented in Figure 1 (I). A total of Twenty discs were prepared; in each group consisting of four samples, 1 for SEM, 1 for confocal and FTIR and 2 for OCT.

2.2. Preparation of copper glass

A Phosphate based glass was prepared using the melt quench process at 1150 ℃ for 90 min in a Pt/5%Au crucible. Phosphorus pentoxide (P_2O_5), calcium carbonate ($CaCO_3$), sodium dihydrogen phosphate (NaH_2PO_4), and copper oxide (CuO) were used as precursors. The molten glass was quenched to room temperature. After cooling, it was ground into powder with particle size of 60 - 200 μm using a ball milling machine (Retsch PM100) [22].

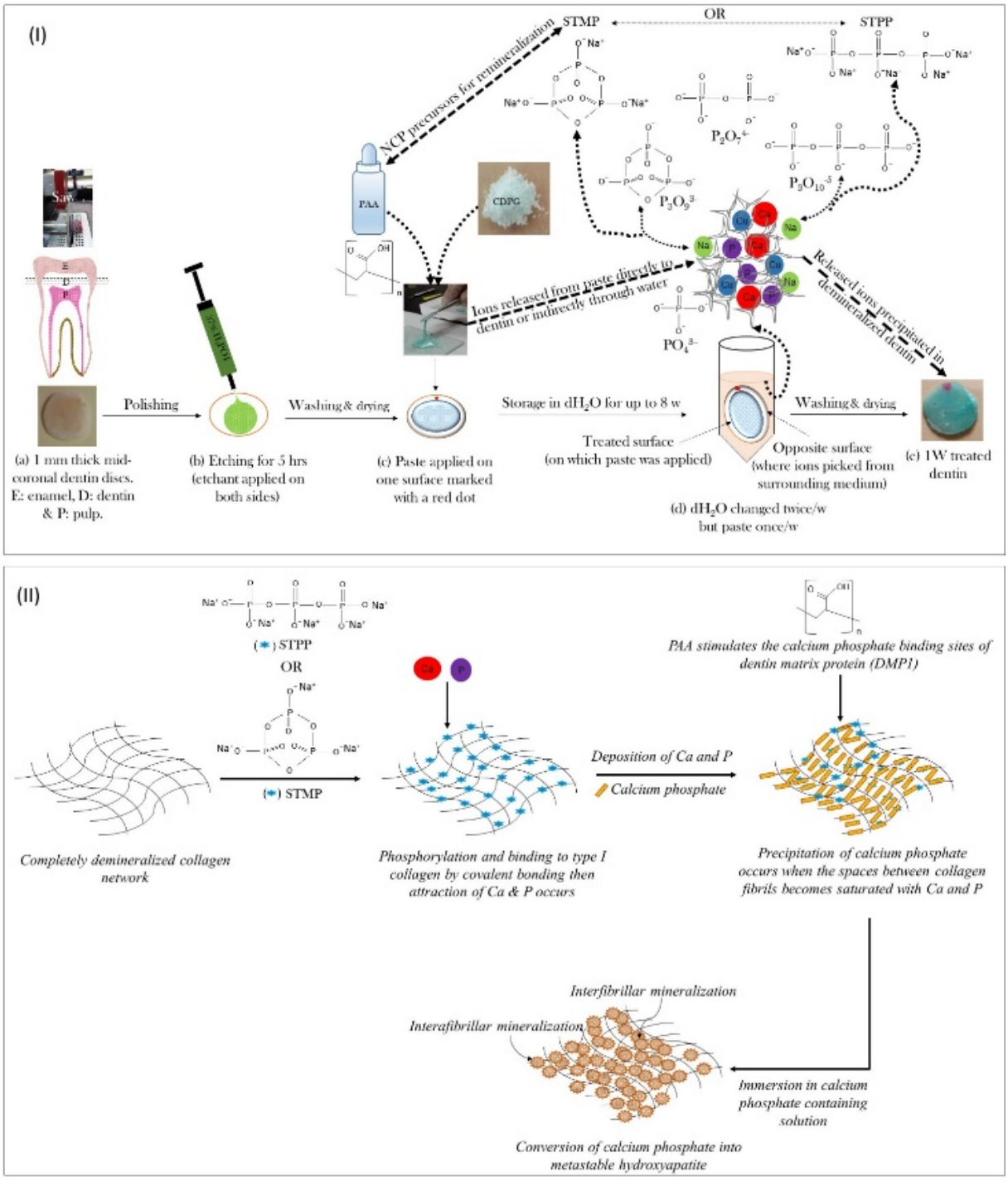

Figure 1: (I) Schematic diagram showing the stages of sample preparation. (II) Proposed mechanism of biomimetic remineralization with PGPAP. PAA: polyacrylic acid. STMP: cyclic sodium trimetaphosphate. STPP: linear sodium tripolyphosphate. NCP: non-collagenous protein. PAA, STMP and STPP are non-collagenous protein precursors required for remineralization.

2.3. Preparation of phosphate glass polyacrylate paste (PGPAP)

To make the paste, the glass powder was mixed with polyacrylic acid (3M ESPE, Germany) at 2:1 ratio. The paste was applied on one surface of the dentin discs which were then immersed in 10 ml of distilled water at 37 °C for up to 8 weeks. The paste was replaced once a week but the water twice a week. After collection, each sample was washed with distilled water to remove the remainder of the paste. The unbound mineral was removed gently using soft tissues. Etched dentin samples, kept in distilled water, were used as controls.

2.4. Confocal laser scanning microscopy (CLSM)

Dentin samples were investigated by CLSM (Olympus LX81 with Fluoview FV1000 scanner software version 4.1) using 473 nm blue laser for excitation, dichroic mirror 405/473/543/ 635 and monochromator set of 480-520 nm wavelengths [25]. The gain of the detector was maintained constant for all images. Specimens were scanned from a pre-set depth, and 3D images were recorded [26] (laser intensity of 50%, raster scanning direction mode from left to right, aspect ratio 1:1, scanning speed of 10 µs/pixels, pixel size X, Y= 512 x 512, numerical aperture 0.90, confocal aperture 235 µm, and 60x water-immersed lens). The recorded images have an approximate theoretical spatial resolution of 0.185 µm and axial resolution of 1.20 µm. Images were then processed using Imaris (CLSM image analyzing software, Bitplane 7.1.0).

2.5. Scanning electron microscopy/energy dispersive X-ray microanalysis (SEM/EDX)

Dried dentin samples were mounted onto aluminum stubs, sputter coated with gold palladium (Polaron E5000 Sputter Coater, Quorum Technologies Ltd, Newhaven, East Sussex, UK) and scanned using SEM (Philips XL30 FEGSEM, Eindhoven, Netherlands) at 5 kV beam, small spot size and working distance of 10 mm. The composition of the precipitate seen on the surface of samples was analysed using EDX (Inca 400 EDX, Oxford Instruments Analytical, High Wycombe, Buckinghamshire, UK) at 20 kV beam and a large spot size.

2.6. Optical coherence tomography (OCT)

A VivoSight Multi-Beam Swept Source OCT system (Michelson Diagnostics Ltd, UK) was used to characterize the cross-section of dentin discs. This system uses a class I laser (λ = 1305 nm) and scans at 10 kHz. The default scanning volume was set to 6 mm x 6 mm and approximately 2 mm deep. For each sample, a total of 500 B-scans were recorded over that volume. Each B-scan was recorded 10 μm apart and with a pixel size of 4.53 μm. Specimens were mounted directly on a glass slide so that the surface of the sample was normal to the incident OCT beam. The samples were not hydrated. Selected B-scans were chosen randomly from each 500 B-scan image stack. Grey scale intensity profiling was conducted by extracting a vertical scattering profile (A-scan) using ImageJ software [27].

2.7. Fourier transform infrared spectroscopy (FTIR)

A PerkinElmer Frontier™ FTIR (USA) equipped with diamond prism ATR accessory was used to collect the spectrum with 16 scan from 450-4000 cm^{-1}.

3. Results

3.1. Confocal laser scanning microscopy (CLSM)

As seen from CLSM in Figure 2, after etching with 37% phosphoric acid for 5 hrs, the dentin was severely demineralized. This can be clearly noted from the extensively open tubules and the changing form and structure of dentinal tubules in some areas. Incubating these dentin samples in distilled water (pH=7) for up to 8 weeks produced no further changes to the dentin surface [Figure 2 (c, e & g)]. In contrast, the application of PGPAP for 1 week on the dentin surface led to a partial occlusion of dentinal tubules [Figure 2 (d)]. The number of occluded dentinal tubules as well as the depth of occlusion increased with increasing the treatment time [Figure 2 (b, f & h)]. After 8 weeks, the occlusion of all tubules was almost complete [Figure 2 (h)].

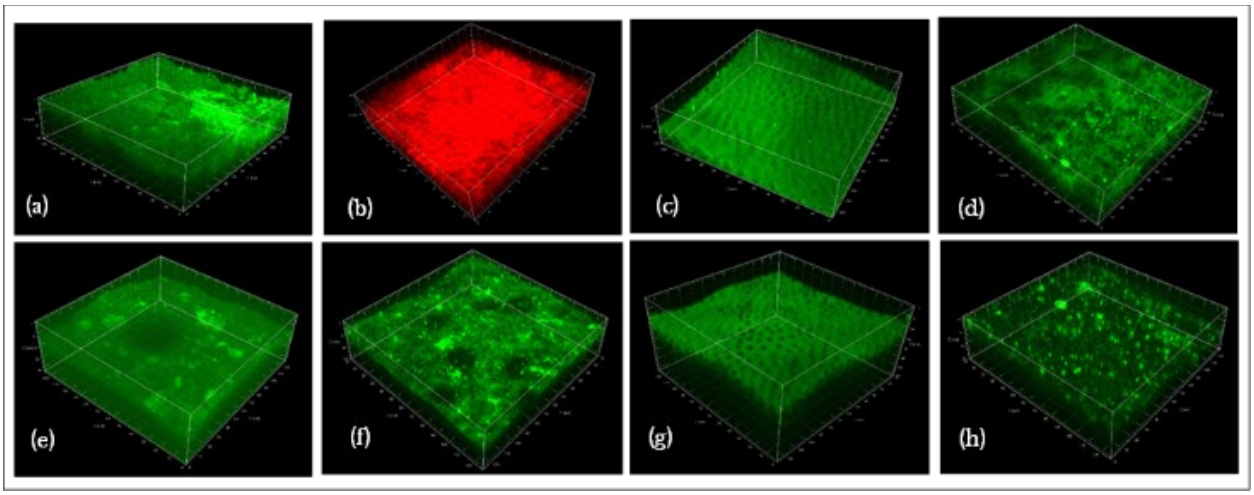

Figure 2: CLSM images showing etched dentin samples kept in distilled water for 1 (a), 2 (c), 4 (e) and 8 weeks (g) and dentin samples treated with the PGPAP for 1 (b), 2 (d), 4 (f) and 8 weeks (h). Etching for 5 hrs completely demineralizes dentin. Remineralization occurs after the application of PGPAP and its depth increases with time until complete remineralization occurs at 8 weeks.

3.2. Scanning electron microscopy/energy dispersive X-ray microanalysis (SEM/EDX)

Electron microscopy images from both occlusal (Figure 3) and lateral orientation (Figure 4) were used to examine the extent of demineralization/remineralization of dentin samples.

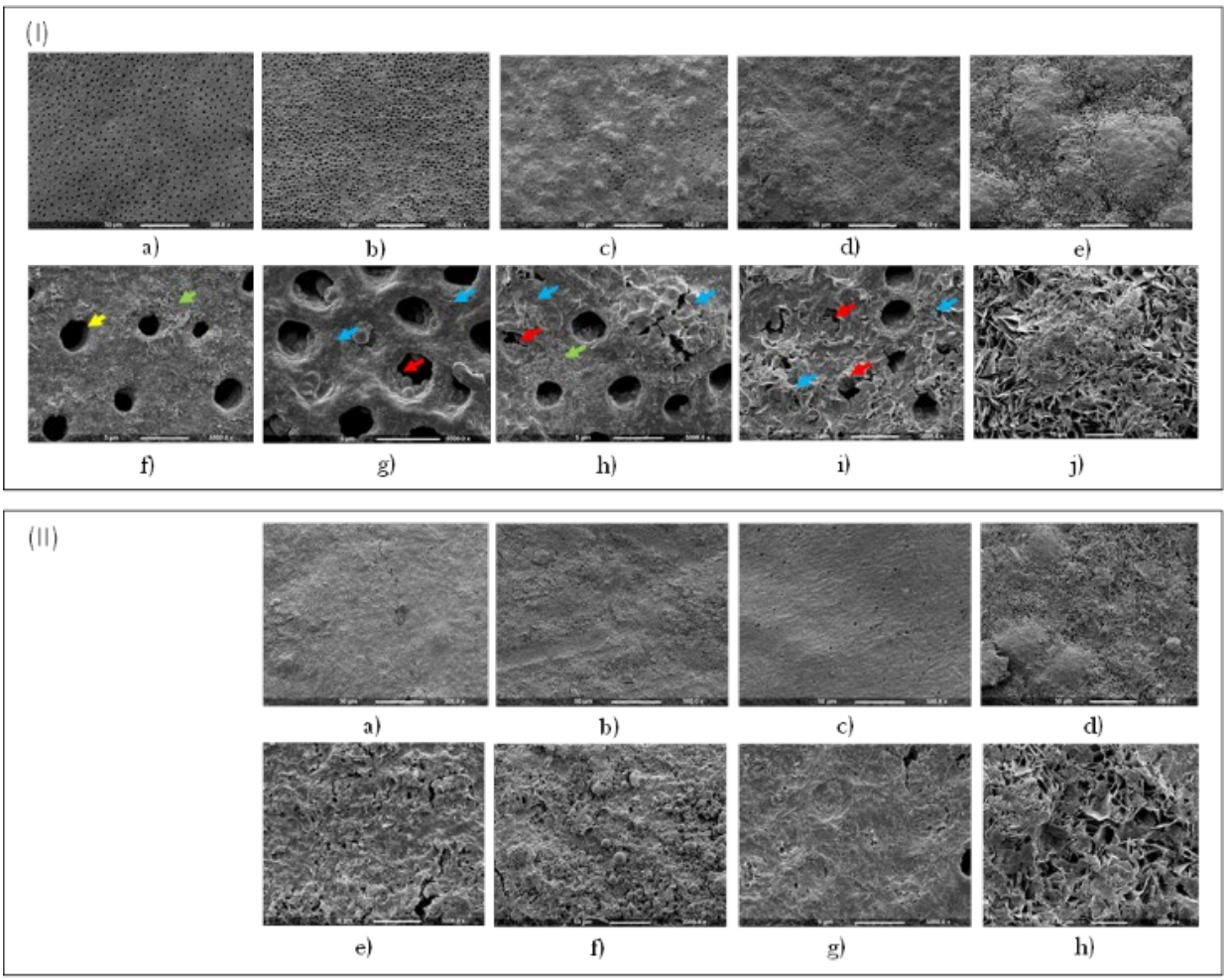

Figure 3: (I) SEM showing: (a & f) occlusal view of a mid-coronal dentin etched with 37% phosphoric acid for 5 hrs. Opened dentinal tubules, indicated by the yellow arrow, were seen after elimination of hydroxyapatite crystals. Fine granules (light green arrows) were seen on the surface of etched dentin; these granules could be the silica gel used to produce the phosphoric acid etchant gel. (b-e & g-j) occlusal view of dentin surface treated with PGPAP at 1, 2, 4 & 8 weeks at low (b-e) and high (g-j) magnification respectively. Deposition of precipitate in inter-tubular dentin (blue arrows) was seen after treatment. Occlusion of the orifices of dentinal tubules (red arrows) was also seen; the level of tubule occlusion increased with increasing the treatment time. Complete occlusion of tubules as well as the remineralization of inter-tubular dentin was seen at 8 weeks (e & j). P: peri-tubular dentin and I: inter-tubular dentin. (II) SEM showing the occlusal view of dentin surface opposite to the treated surface (ie surface not in direct contact with the paste) after 1, 2, 4 & 8 weeks respectively at both low (a-d) and high (e-h) magnification. These surfaces showed nearly complete occlusion of dentinal tubules.

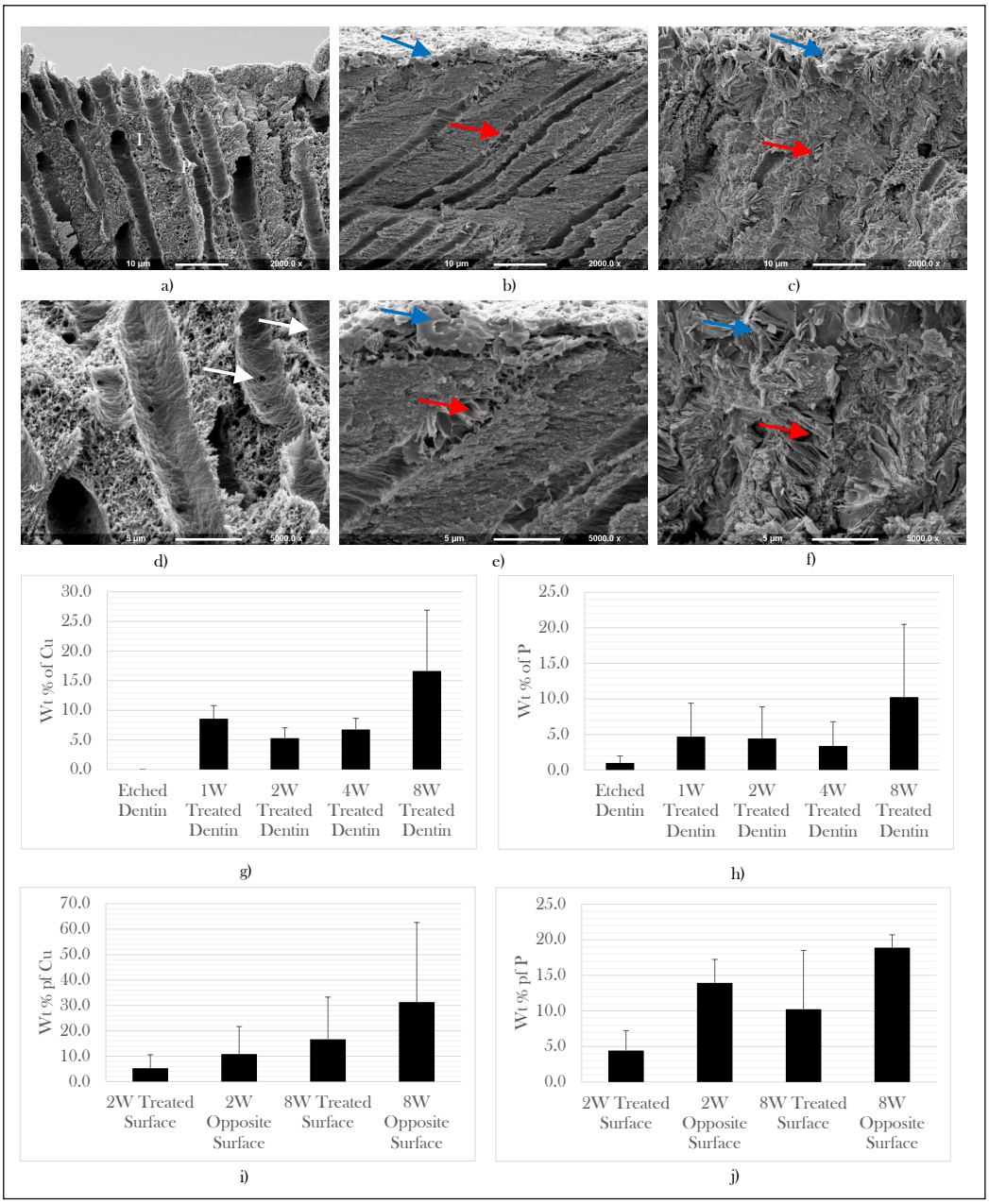

Figure 4: SEM showing the lateral view of dentin: control (etched & kept in distilled water) (a & d), treated for 2 weeks (b & e) and 8 weeks (c & f) at low and high magnification respectively. Individualized collagen fibrils, indicated by white arrows, were seen within the walls of dentinal tubules (a & d). For treated dentin, however, crystalline precipitates were seen on the surface of dentin (ie, in inter-tubular dentin and sealing the orifices of dentinal tubules (blue arrows) as well as in the lumen of dentinal tubules (red arrows). The lumen of dentinal tubules was reduced by the deposition of crystalline precipitates at 2 weeks; complete occlusion (plugging) of tubules, however, occurred at 8 weeks. From EDX analysis, weight % of Cu and P increased with time (g & h). Cu & P are also present in high wt% on the surface opposite to the treated ones (i & j). P: peri-tubular dentin and I: inter-tubular dentin.

The occlusal orientation images were recorded for both the treated surface (the surface upon which the paste was applied) [Figure 3 (I)] as well as the opposing surface (ie, surface not in direct contact with the paste but indirectly received ions from the paste through the incubating medium) [Figure 3 (II)]. After etching with 37% phosphoric acid for 5 hrs, the dentin surface did not present any signs of smear layer (debris produced during tooth cutting) and the all dentinal tubules were clearly opened [Figure 3 (I) a] as observed from CLSM. The diameter of these tubules varied from 2-4 μm. In 200 μm^2 area, the number of patent dentinal tubules was $N_{initial}$=183±5. Collagen fibrils were not detected in inter-tubular or peri-tubular dentin. A small amount of precipitate could be seen on the inter-tubular dentin (green arrows) [Figure 3 (I) f]. Occlusion of dentinal tubules, indicated by red arrows, was observed after treating dentin surface with PGPAP - Figure 3 (I). The number of occluded tubules increased with the treatment time as observed from CLSM. After 4 weeks of treatment, the number of patent dentinal tubules in 200 μm^2 is N_{4weeks} 35±5. This means that the number of patent tubules was reduced by five times when compared with etched dentin [Figure 3 (I) d & i]. Nearly all tubules' orifices were completely occluded with angular-like crystals after 8 weeks [Figure 3 (I) e & j]. These crystals also precipitated on the inter-tubular dentin (blue arrows); the whole dentin surface was completely covered with these crystals at 8 weeks. This corroborates the findings from CLSM. Looking at the dentin surface opposing the treated side – Figure 3 (II), the surface was completely covered with precipitated crystals at every studied time point. The crystalline nature of the precipitate was clearly demonstrated on the 8th week samples [Figure 3 (II) h]. In this case, the ions released from CDPG into the medium were precipitated onto the dentin surface.

The cross-sectional view of the dentin disc showed the lumen of the dentinal tubules – Figure 4. As for the etched dentin disc kept in distilled water, the lumen of the tubules was opened [Figure

4 (a & d)]. Peri-tubular fibrillar arrangement of the collagen fibrils can also be observed in Figure 4 (d). However, for the dentin discs treated with PGPAP, the lumen became increasingly obturated and reduced in diameter as seen for samples treated for 2 weeks as an example – [Figure 4 (b & e)]. The lumen of the dentinal tubules was completely occluded with precipitated crystals after 8 weeks – [Figure 4 (c & f)].

EDX showed the elemental composition of the precipitate seen on surface of treated dentin. For etched dentin, there was no Cu detected as expected. The highest level of Cu was recorded at 8 weeks, but it varies highly across the sample – [Figure 4 (g)]. Treated dentin also showed higher weight % of P than etched dentin – [Figure 4 (h)]. As observed the weight % of Cu and P increased with time. Looking at the surface opposing the treated one, higher weight % of Cu and P was detected than those on the treated surface – [Figure 4 (i & j)].

3.3. Optical coherence tomography (OCT)

Etched dentin showed the presence of a much pitted, heterogeneous demineralized surface. The depth of the frayed and fully demineralized surface layer is 120±30μm. Some deep large holes, originating from the surface, of approximately 200μm. These holes are too large to be associated with dentin tubules and would be most likely associated with surface breakdown. Sub-surface partial demineralization was also observed at a depth ranging from 100-300μm. Figure 5 presents a selection of randomly selected B-scans obtained respectively from the dentin discs exposed to PGPAP for 1 week [Figure 5 (a)], 2 weeks [Figure 5 (b)] and 8 weeks [Figure 5 (c)] with their associated scattering profiles also known as A-scans [Figure 5 (d)].

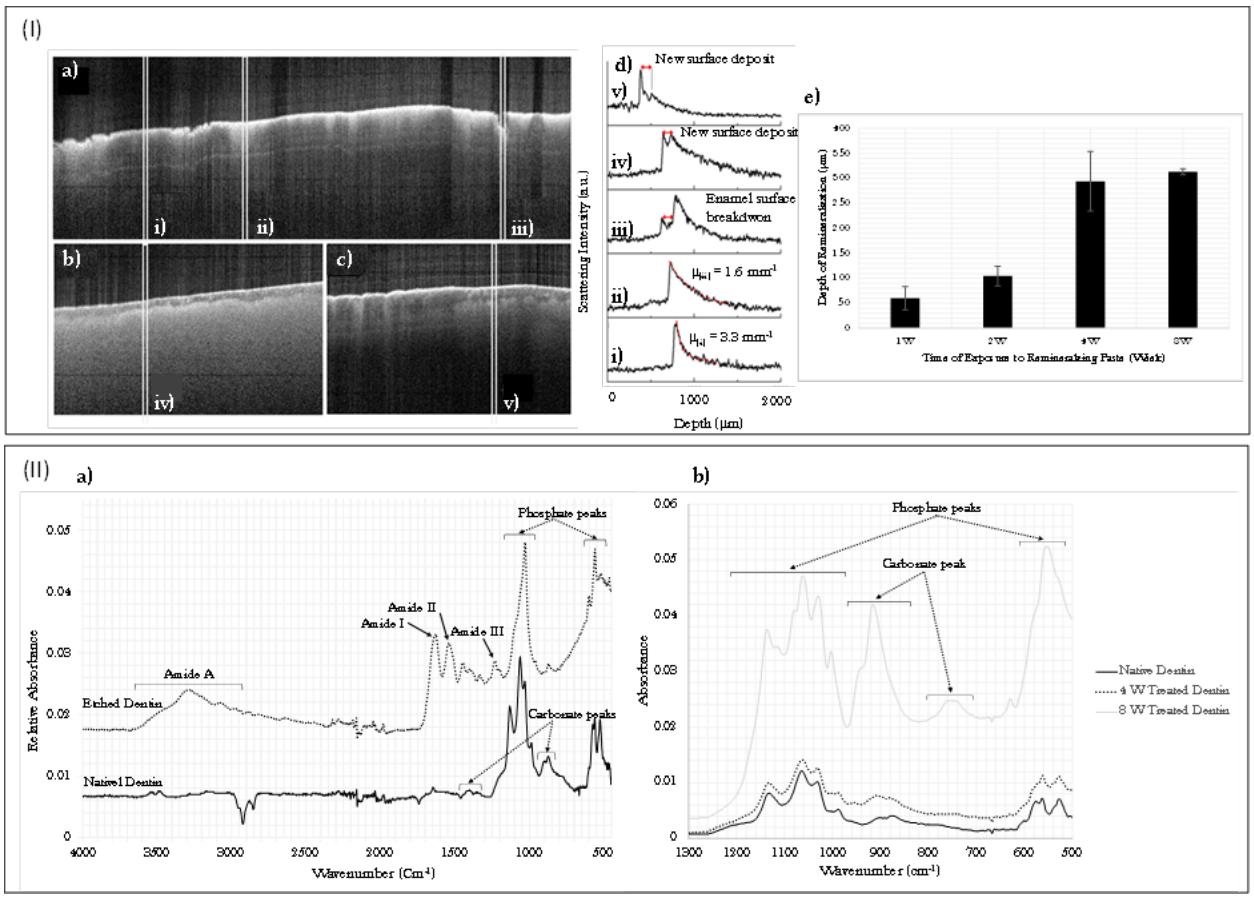

Figure 5: (I) A selection of randomly selected B-scans obtained respectively from the dentin discs exposed to treatment for 1 week (a), 2 weeks (b) and 8 weeks (c) with their associated A-scans (d). Overall, the surface topology of 1week sample appears inhomogeneous, with several areas pitted and frayed. This roughened layer was then covered with a fairly homogenous layer after 2 and 8 weeks of treatment. The depth of this layer increased as a function of treatment time (e). (II) FTIR spectra of native versus etched dentin (a) as well as dentin samples treated with PGPAP versus native dentin (b). Etching demineralizes dentin as indicated by the appearance of amid peaks from collagen. Lost phosphate peaks were restored after treatment with the experimental past. 4 weeks samples have a spectrum consistent with that for native dentin. 8 weeks samples, however, have stronger phosphate and carbonate peaks than native dentin.

In Figure 5 (a), three regions of interests have been selected to present various elements of the surface demineralization. Overall, the surface topology of the sample appears inhomogeneous, with several areas pitted and frayed. The cross-sectional scattering image presents signs of

subsurface demineralization as reflected by an inhomogeneous grey-scale contrast close to the dentin-air interface.

The first region of interest (i) presents a uniform scattering throughout the dentin cross-section as illustrated through its representative A-scans. However, region (ii) presents a higher degree of scattering as the area immediately below the air-dentin interface has become significantly brighter in contrast. Using the approach described by Ueno et al [28], the attenuation coefficient (μ) of A-scan signal was measured for both i) and ii) yielded respectively values of $\mu_{(i)}=3.3mm^{-1}$ and $\mu_{(ii)}=1.6mm^{-1}$. In the case of the less demineralised ROI, the attenuation coefficient is greater than that of the more demineralised ROI. In the region (iii), the A-scan signal presents a fingerprint of a surface breakdown as a result of the surface erosion, with a significant proportion of the surface dentin missing. In these images, the surface appearance of the dentin has changed significantly when compared to Figure 5 (a). A surface layer can be observed above the roughened dentin surface - Figure 5 (b and c). It is very likely this surface layer would be the result of the treatment. The layer appears fairly homogenous on the B-scan presented but has more variation in thickness throughout the entire area imaged. The thickness of the deposited layer was measured directly on the A-scan signals by monitoring the position of the main scattering peak related to the air-layer interface and the second strongest peak which was associated with the layer-dentin interface.

The thickness of surface deposits seen on treated dentin (depth of remineralization) increased with increasing the time of exposure to the remineralizing paste. The depth of remineralization was nearly doubled after 2 weeks (105±20μm). After 4 weeks, however, it increased to 294±60μm. After 8 weeks, the depth of remineralized layer reached 313±6μm ie, nearly all demineralized dentin becomes remineralized [Figure 5 (e)].

3.4. Fourier transform infrared spectroscopy (FTIR)

FTIR showed that native dentin characterized by the presence of phosphate peaks at 1188-940 and 650-490 cm^{-1} and carbonate peaks at 1490-1310 and 940-830 cm^{-1} [29] – [Figure 5 (II) a]. Amide peaks of collagen could also be observed but with low intensity. Etching with phosphoric acid demineralizes dentin as indicated by the appearance of amid peaks from collagen. Amide I, II and III peaks were detected at 1760-1595 cm^{-1}, 1595-1490 cm^{-1}, 1290-1185 cm^{-1} respectively while amide A was seen at 3698-2780 cm^{-1} [29]. Some phosphate, corresponding to PO_4^{3-} in a poorly crystalline apatite, was also detected in etched dentin as also seen from EDX – Figure 4 (g and h) and the deposits seen from SEM – [Figure 3 (I) f]. Treatment of dentin with the experimental paste replaced the phosphate lost due to etching – [Figure 5 (II) b]. The FTIR spectrum of dentin treated for 4 weeks was consistent with that for native dentin. The FTIR spectrum of dentin treated for 8 weeks, however, showed higher intensity of both phosphate and carbonate (940-830[29] & 804-705 cm^{-1} [30]) peaks than those for native dentin.

4. Discussion

Dentin is a complex tissue; it has ~70 wt% carbonated apatite, 20 wt% proteins (mainly collagen, non-collagenous proteins and glycoproteins) and 10 wt% H_2O. Demineralization and remineralization of teeth are lifelong dynamic processes [31]. Unlike bones, dentin does not undergo self-repair via the synergetic activities of osteoclasts and osteoblasts cells. A sustained extrinsic demineralization is one of the causative reasons for dental caries to occur and the main mechanism for the dentin tissue to break down during those carious events. One of the challenges facing restorative and preventive dentistry is to remineralize hypomineralized carious dentin.

As seen from CLSM, after etching with 37% phosphoric acid for 5 hrs, the dentin was severely demineralized as noted from the extensively open tubules and altered form and structure of dentinal tubules in some areas. The excessive exposure of the dentin to phosphoric acid (when compared to previous studies [16, 32]) was found to replicate affected dentin, in which the collagen matrix is not just partially demineralized but has also been partially exposed and degraded due to bacteria-released acetic acid. Occlusion of dentinal tubules that almost completed after 8 weeks of treatment with glass polyacrylate paste could indicate a significant remineralization had occurred even though samples were kept in unfavorable mineralization buffer (demineralized water). As a result of ions diffusion into dentin, as an indication of remineralization, the color of the dentin samples varied greatly between pre and post treatment with PGPAP. The green-tint observed on the sample was expected due to the diffusion of copper ions, released from CDPG [19], into dentin as confirmed by EDX. The non-uniformity of Cu distribution across the sample surface, however, could be due to the static condition in which the samples were kept during the experimental period. The green-tint was observed on both sides of dentin samples even though the paste was applied on one side only. The presence of copper oxide was intentionally used in the glass so that ion diffusion into dentin can be visually observed. Other oxides eg, zinc [33], gallium [34] and titanium oxide [35, 36] could be used as alternatives in the future work without the fear of tooth discoloration.

As observed using SEM, collagen fibrils were not detected in inter-tubular or peri-tubular dentin of etched dentin; this could be due to the collapse of fibrils caused by the critical drying used during sample preparation for SEM [37]. The precipitate seen on the inter-tubular dentin could be the silica gel particles used by manufacturers to produce phosphoric acid etchant gel [38] or calcium phosphate precipitated after being removed from dentin. Regardless of absence of the mineral phase of etched dentin, as indicated from CLSM and SEM, remineralization of collagen,

the major component of dentin matrix, has occurred. This might indicate that the intermolecular cross-links and cross-banding pattern of collagen has not been severely affected by acid etching [39]. Collagen serves as a scaffold for mineral deposition but does not provide a mechanism for nucleation [40]. Phosphate species, released during CDPG degradation, however could play a key role in guiding nucleation and crystals growth within the spaces between collagen fibrils during biomimetic remineralization [15]. These phosphate species include orthophosphate (PO_4^{3-}), cyclic trimetaphosphate ($P_3O_9^{3-}$), pyrophosphate ($P_2O_7^{4-}$) and linear polyphosphate ($P_3O_{10}^{-5}$) – Figure 1 (I). The highest release was observed for trimetaphosphate ($P_3O_9^{3-}$) that represents the main phase in the original glass [41]. Since CDPG also releases Na [41], each $P_3O_9^{3-}$ species can be easily combined with three Na^+ ions to form sodium trimetaphosphate (STMP) complexes – Figure 1 (I). This could explain the biomimetic remineralization potential of PGPAP since STMP has been proven as a biomimetic analogue of matrix phosphoproteins for remineralization of artificial caries-like dentin [15]. STMP acts by phosphorylation and binding to type I collagen by covalent bonding (mainly to amino acids in collagen with OH group eg, serine [24]). The phosphorylated amino acids act as templates for the attraction of Ca and phosphate [15, 20, 24]. When the spaces between collagen fibrils becomes supersaturated with Ca and phosphate, their precipitation starts to occur – Figure 1 (II). The conversion of calcium phosphate into a thermodynamically stable hydroxyapatite will occur [42].

It has been suggested by some authors [24, 43] that phosphorylation of collagen with STMP requires its hydrolysis to linear sodium tripolyphosphate form (STPP). Conversion of STMP to STPP requires alkaline hydrolysis of STMP in presence of sodium hydroxide and high pH (12). As mentioned above, linear tripolyphosphate (P_3O_{10}) is also released during CDPG degradation and can easily bind to 5 Na atoms that will be released during degradation (ie, no need for pH

adjustment). Not only STMP but also PAA has been used as non-collagenous protein (NCP) precursor in dentin remineralization [15, 24]. PAA stimulates the calcium phosphate binding sites of dentin matrix protein (DMP1) [15, 24] – Figure 1 (II). Therefore, phosphate glass polyacrylate paste used in this study has two important NCP precursors (STMP and PAA) that facilitate the biomimetic remineralization of collagen.

The lumen of dentinal tubules was completely occluded with the precipitated crystals after 8 weeks. This process is reminiscent to the formation of sclerotic dentin in the advancing front of demineralized dentin as a protective mechanism offered by the vital pulp where the crystalline precipitates completely occlude the lumen of affected dentinal tubules [44, 45]. Occlusion of dentinal tubules could also reduce fluid movement and hence reduce the postoperative sensitivity seen with most restorative procedures and materials [46]. After 8 weeks' exposure, it becomes difficult to differentiate the occluded tubules from the inter-tubular dentin which supports the concept of complete remineralization in the upper section of the tubules. The mineralized deposit is structurally similar to brushite, presenting a staggered arrangement of mineralized platelets [47]. Additionally, there is no delamination of the deposited layers under vacuum, used for SEM, which suggests a strong adhesion or binding of this layer to the now remineralized dentin. This is further supported by the occlusion of the dentin tubules that would act as "resin" tag for this layer as commonly found in composite restorations.

The depth of demineralization/remineralization of etched/treated dentin was detected using Optical Coherence Tomography. OCT is becoming more and more popular in dentistry especially in caries detection and management, tooth fracture diagnosis and finally in the detection of gap formation and secondary caries at the restoration–tooth interface [28, 48]. Even though, there was no

significant difference in depth of remineralization between 8 and 4 weeks; the deviation in the thickness of the remineralization layer after 8 weeks was reduced significantly from 60 to 6μm inferring that the mineralization process evened out over that period.

The chemistry of dentin surface was studied by FTIR. Etching with phosphoric acid demineralizes dentin as indicated by the appearance of amid peaks from collagen and the presence of poorly crystalline apatite. This finding confirms that the crystals seen on surface of etched dentin are actually calcium phosphate precipitated after being removed by etching. Treatment of dentin with the experimental paste replaced the phosphate lost as a result of etching and the structure went back to native dentin after 4 weeks of treatment. After 8 weeks of treatment, the higher intensity of both phosphate and carbonate peaks than those for native dentin might indicate the continuation of remineralization process. The increased intensity of phosphate peaks is consistent with the intake of both Ca and P released from CDPG. The increased intensity of carbonate peak, however, could be correlated with the intake of Cu and then its interaction with carbonate especially the highest Cu detection was observed for 8 week treated samples.

5. Conclusion

After further extensive improvement and thorough characterization, due to its biomimetic remineralization potential, this dual-analogue paste might offer a solution for in-situ recapitulation of the original dentin properties towards a pre-carious (native) status. Examples of potential applications of this paste might include remineralization of affected dentin kept after minimal invasive caries removal. Another potential application might include remineralizing dentin exposed to deep acid etching; this will help strengthen the bonded interface and improve the longevity of restorations [49]. Testing the antibacterial action of this paste against oral biofilm

using a constant depth film fermenter model will be considered in future work. When designing this experiment, the dynamics of oral environment in term of carbohydrate level and the presence of saliva will be considered. Change in surface topography of dentin and its effect on bonding with materials will be also investigated.

Acknowledgement

The authors would like to acknowledge Basant E. Katamesh for English editing.

Notes

The authors declare no competing financial interests.

REFERENCES

1. Holmgren CJ, Roux D, Doméjean S. Minimal intervention dentistry: part 5. Atraumatic restorative treatment (ART) – a minimum intervention and minimally invasive approach for the management of dental caries. Bdj. 2013;214:11.
2. Borges BC, de Souza Borges J, de Araujo LS, Machado CT, Dos Santos AJ, de Assuncao Pinheiro IV. Update on nonsurgical, ultraconservative approaches to treat effectively non-cavitated caries lesions in permanent teeth. European journal of dentistry. 2011;5(2):229-36. Epub 2011/04/16.
3. Li-na Niu WZ, David H. Pashley, Lorenzo Breschi, Jing Mao, Ji-hua Chen and Franklin R. Tay. Biomimetic remineralization of dentin. Dent Mater 2014;30(1):1-35.
4. JM. TC. In vitro studies on the effects of fluoride on de-and remineralization. J Dent Res 1990 69:614-9.
5. Hernandez M, Cobb D, Swift EJ, Jr. Current strategies in dentin remineralization. Journal of esthetic and restorative dentistry : official publication of the American Academy of Esthetic Dentistry [et al]. 2014;26(2):139-45. Epub 2014/03/13.
6. R1 V, DE, GA, MJ, GE. Biomimetic Approaches of Dentin Regeneration. International Journal of Science and Research (IJSR) 2013;6(14):752-5.
7. Creanor SL, Awawdeh LA, Saunders WP, Foye RH, Gilmour WH. The effect of a resin-modified glass ionomer restorative material on artificially demineralised dentine caries in vitro. Journal of dentistry. 1998;26(5-6):527-31. Epub 1998/08/12.
8. Niu LN, Zhang W, Pashley DH, Breschi L, Mao J, Chen JH, et al. Biomimetic remineralization of dentin. Dental materials : official publication of the Academy of Dental Materials. 2014;30(1):77-96.
9. Sangwan P, Sangwan A, Duhan J, Rohilla A. Tertiary dentinogenesis with calcium hydroxide: a review of proposed mechanisms. Int Endod J 2013 Jan;46(1):3-19 doi: 101111/j1365-2591201202101x Epub 2012 Aug 13.
10. Kaur M, Singh H, Dhillon JS, Batra M, Saini M. MTA versus Biodentine: Review of Literature with a Comparative Analysis. Journal of clinical and diagnostic research : JCDR. 2017;11(8):Zg01-zg5. Epub 2017/10/04.
11. Malkondu O, Karapinar Kazandag M, Kazazoglu E. A review on biodentine, a contemporary dentine replacement and repair material. BioMed research international. 2014;2014:160951. Epub 2014/07/16.
12. Koubi G, Colon P, Franquin JC, Hartmann A, Richard G, Faure MO, et al. Clinical evaluation of the performance and safety of a new dentine substitute, Biodentine, in the restoration of posterior teeth - a prospective study. Clinical oral investigations. 2013;17(1):243-9. Epub 2012/03/14.
13. Huang XQ, Camba J, Gu LS, Bergeron BE, Ricucci D, Pashley DH, et al. Mechanism of bioactive molecular extraction from mineralized dentin by calcium hydroxide and tricalcium silicate cement. Dental materials : official publication of the Academy of Dental Materials. 2018;34(2):317-30. Epub 2017/11/29.
14. Forsback AP, Areva S, Salonen JI. Mineralization of dentin induced by treatment with bioactive glass S53P4 in vitro. Acta odontologica Scandinavica. 2004;62(1):14-20. Epub 2004/05/06.
15. Liu Y, Li N, Qi Y, Niu LN, Elshafiy S, Mao J, et al. The use of sodium trimetaphosphate as a biomimetic analog of matrix phosphoproteins for remineralization of artificial caries-like dentin. Dental materials : official publication of the Academy of Dental Materials. 2011;27(5):465-77. Epub 2011/03/01.

16. Xu Z, Neoh KG, Lin CC, Kishen A. Biomimetic deposition of calcium phosphate minerals on the surface of partially demineralized dentine modified with phosphorylated chitosan. Journal of biomedical materials research Part B, Applied biomaterials. 2011;98(1):150-9. Epub 2011/05/04.
17. AR Prabhakar, Jibi Paul M, Basappa N. Comparative Evaluation of the Remineralizing Effects and Surface Microhardness of Glass Ionomer Cements Containing Bioactive Glass (S53P4): An in vitro Study. International Journal of Clinical Pediatric Dentistry. 2010;3(2):69-77.
18. Abou Neel EA, Young AM, Nazhat SN, Knowles JC. A facile synthesis route to prepare microtubes from phosphate glass fibres. Advanced Materials 2007;19(19):2856-62.
19. Abou Neel EA, Kiani A, Valappil SP, Mordan NM, Baek S-Y, Hossain KMZ, et al. Glass microparticle- versus microsphere-filled experimental dental adhesives. J Appl Polym Sci 2019;136: 47832.
20. Cao CY, Mei ML, Li QL, Lo EC, Chu CH. Methods for biomimetic remineralization of human dentine: a systematic review. International journal of molecular sciences. 2015;16(3):4615-27. Epub 2015/03/05.
21. Abou Neel EA, Pickup DM, Valappil SP, Newport RJ, Knowles JC. Bioactive functional materials: a perspective on phosphate-based glasses. Journal of Materials Chemistry. 2009;19(6):690-701.
22. Abou Neel EA, Ahmed I, Pratten J, Nazhat SN, Knowles JC. Characterisation of antibacterial copper releasing degradable phosphate glass fibres. Biomaterials. 2005;26(15):2247-54. Epub 2004/12/09.
23. Sauro S, Faus-Matoses V, Makeeva I, Manuel Nuñez Martí J, Gonzalez Martínez R, Antonio García Bautista J, et al. Effects of polyacrylic acid pre-treatment on bonded-dentine interfaces created with a modern bioactive resin-modified glass ionomer cement and subjected to cycling mechanical stress2018. 1884 p.
24. Gu L, Kim YK, Liu Y, Ryou H, Wimmer CE, Dai L, et al. Biomimetic analogs for collagen biomineralization. Journal of dental research. 2011;90(1):82-7.
25. Pioch T, Stotz S, Staehle HJ, Duschner H. Applications of confocal laser scanning microscopy to dental bonding. Advances in dental research. 1997;11(4):453-61. Epub 1998/02/21.
26. Evans A, Harper I, Sanson G. Confocal imaging, visualization and 3-D surface measurement of small mammalian teeth2001. 108-18 p.
27. Schneider CA, Rasband WS, Eliceiri KW. NIH Image to ImageJ: 25 years of image analysis. Nature methods. 2012;9(7):671-5. Epub 2012/08/30.
28. Ueno T SY, Matin K, Zhou Y, Wada I, Sadr A, Sumi Y, Tagami J. Optical analysis of enamel and dentin caries in relation to mineral density using swept-source optical coherence tomography. J Med Imaging (Bellingham). 2016;3(33):035507.
29. Morgan AD, Ng YL, Odlyha M, Gulabivala K, Bozec L. Proof-of-concept study to establish an in situ method to determine the nature and depth of collagen changes in dentine using Fourier Transform Infra-Red spectroscopy after sodium hypochlorite irrigation. International endodontic journal. 2019;52(3):359-70. Epub 2018/08/26.
30. El Feki H, Rey C, Vignoles M. Carbonate ions in apatites: Infrared investigations in thev4 CO3 domain. Calcified Tissue International. 1991;49(4):269-74.
31. Abou Neel EA, Aljabo A, Strange A, Ibrahim S, Coathup M, Young AM, et al. Demineralization-remineralization dynamics in teeth and bone. International journal of nanomedicine. 2016;11:4743-63.
32. Zhang X, Neoh KG, Lin CC, Kishen A. Remineralization of partially demineralized dentine substrate based on a biomimetic strategy. J Mater Sci Mater Med. 2012;23(3):733-42. Epub 2012/01/25.
33. Abou Neel EA, O'Dell LA, Smith ME, Knowles JC. Processing, characterisation, and biocompatibility of zinc modified metaphosphate based glasses for biomedical applications. J Mater Sci Mater Med. 2008;19(4):1669-79. Epub 2007/12/07.
34. Valappil SP, Ready D, Abou Neel EA, Pickup DM, O'Dell LA, Chrzanowski W, et al. Controlled delivery of antimicrobial gallium ions from phosphate-based glasses. Acta Biomater. 2009;5(4):1198-210. Epub 2008/11/01.
35. Abou Neel EA, O'Dell LA, Chrzanowski W, Smith ME, Knowles JC. Control of surface free energy in titanium doped phosphate based glasses by co-doping with zinc. Journal of biomedical materials research Part B, Applied biomaterials. 2009;89(2):392-407. Epub 2008/10/08.
36. Abou Neel EA, Chrzanowski W, Knowles JC. Effect of increasing titanium dioxide content on bulk and surface properties of phosphate-based glasses. Acta Biomater. 2008;4(3):523-34. Epub 2008/02/06.
37. Irmak Ö, Baltacıoğlu İH, Ulusoy N, Bağış YH. Solvent type influences bond strength to air or blot-dried dentin. BMC oral health. 2016;16(1):77-.
38. Perdigao J, Denehy GE, Swift EJ, Jr. Silica contamination of etched dentin and enamel surfaces: a scanning electron microscopic and bond strength study. Quintessence international (Berlin, Germany : 1985). 1994;25(5):327-33. Epub 1994/05/01.
39. Nakornchai S, Atsawasuwan P, Kitamura E, Surarit R, Yamauchi M. Partial biochemical characterisation of collagen in carious dentin of human primary teeth. Archives of oral biology. 2004;49(4):267-73. Epub 2004/03/09.
40. Gajjeraman S, Narayanan K, Hao J, Qin C, George A. Matrix macromolecules in hard tissues control the nucleation and hierarchical assembly of hydroxyapatite. The Journal of biological chemistry. 2007;282(2):1193-204. Epub 2006/10/21.
41. Abou Neel EA. Collagen-phosphate glass fibres for biomedical and tissue engineering applications. PhD thesis 2006;University of London.
42. Eanes ED. Octacalcium phosphate. Monogr Oral Sci 2001;18(130–147).
43. Zhang K, Li Y, Ren Y. Research on the phosphorylation of soy protein isolate with sodium tripoly phosphate. Journal of Food Engineering. 2007;79(4):1233-7.
44. Heymann HO, Edward J. Swift J, Ritter AV. Strudevant's Art and Science of Operative Dentistry: Chapter 2: Dental Caries: Etiology, Clinical Characteristics, Risk Assessment and Management. Strudevant's, editor: Elsevier; 2013.
45. Yoshihara K, Nagaoka N, Nakamura A, Hara T, Hayakawa S, Yoshida Y, et al. Three-dimensional observation and analysis of remineralization in dentinal caries lesions. Scientific Reports. 2020;10(1):4387.
46. Davari A, Ataei E, Assarzadeh H. Dentin hypersensitivity: etiology, diagnosis and treatment; a literature review. Journal of dentistry (Shiraz, Iran). 2013;14(3):136-45.
47. Toshima T, Hamai R, Tafu M, Takemura Y, Fujita S, Chohji T, et al. Morphology control of brushite prepared by aqueous solution synthesis. Journal of Asian Ceramic Societies. 2014;2(1):52-6.
48. Yasushi Shimada AS, Yasunori Sumi, and Junji Tagami. Application of Optical Coherence Tomography (OCT) for Diagnosis of Caries, Cracks, and Defects of Restorations. Curr Oral Health Rep 2015;2(2): 73–80.
49. Tao S, He L, Xu HHK, Weir MD, Fan M, Yu Z, et al. Dentin remineralization via adhesive containing amorphous calcium phosphate nanoparticles in a biofilm-challenged environment. Journal of dentistry. 2019;89:103193.